EUROPEAN JOURNAL OF CANCER 42 (2006) 3294–3303

available at www.sciencedirect.com

journal homepage: www.ejconline.com

Development of luciferase tagged brain tumour models in mice for chemotherapy intervention studies

E.M. Kemper[a], W. Leenders[b], B. Küsters[b], S. Lyons[c], T. Buckle[a], A. Heerschap[d], W. Boogerd[e,f] J.H. Beijnen[f,g,h], O. van Tellingen[a,]*

[a]*Department of Clinical Chemistry, The Netherlands Cancer Institute/Antoni van Leeuwenhoek Huis, Plesmanlaan 121, 1066 CX Amsterdam, The Netherlands*
[b]*Department of Pathology, Radboud University Nijmegen Medical Centre, P.O. Box 9101, 6500 HB Nijmegen, The Netherlands*
[c]*Xenogen Corporation, 860 Atlantic Avenue, Alameda, CA 94501, USA*
[d]*MRI Facility, Radboud University Nijmegen Medical Centre, P.O. Box 9101, 6500 HB Nijmegen, The Netherlands*
[e]*Department of Neurology, Slotervaart Hospital, Louwesweg 6, 1066 EC Amsterdam, The Netherlands*
[f]*Department of Medical Oncology, The Netherlands Cancer Institute/Antoni van Leeuwenhoek Huis, Plesmanlaan 121, 1066 CX Amsterdam, The Netherlands*
[g]*Department of Pharmacy and Pharmacology, The Netherlands Cancer Institute/Slotervaart Hospital, Louwesweg 6, 1066 EC Amsterdam, The Netherlands*
[h]*Division of Drug Toxicology, Faculty of Pharmaceutical Sciences, Utrecht University, Sorbonnelaan 16, 3584 CA Utrecht, The Netherlands*

ARTICLE INFO

Article history:
Received 22 July 2006
Accepted 26 July 2006
Available online 5 October 2006

Keywords:
Brain tumour
Orthotopic xenograft
Animal model

ABSTRACT

The blood–brain barrier (BBB) is considered one of the major causes for the low efficacy of cytotoxic compounds against primary brain tumours. The aim of this study was to develop intracranial tumour models in mice featuring intact or locally disrupted BBB properties, which can be used in testing chemotherapy against brain tumours. These tumours were established by intracranial injection of suspensions of different tumour cell lines. All cell lines had been transfected with luciferase to allow non-invasive imaging of tumour development using a super-cooled CCD-camera. Following their implantation, tumours developed which displayed the infiltrative, invasive or expansive growth patterns that are also found in primary brain cancer or brain metastases. Contrast-enhanced magnetic resonance imaging showed that the Mel57, K1735Br2 and RG-2 lesions grow without disruption of the BBB, whereas the BBB was leaky in the U87MG and VEGF-A-transfected Mel57 lesions. This was confirmed by immunohistochemistry. Bioluminescence measurements allowed the visualisation of tumour burden already within 4 days after injection of the tumour cells. The applicability of our models for performing efficacy studies was demonstrated in an experiment using temozolomide as study drug. In conclusion, we have developed experimental brain tumour models with partly disrupted, or completely intact BBB properties. *In vivo* imaging by luciferase allows convenient follow-up of tumour growth and these models will be useful for chemotherapeutic intervention studies.

* *Corresponding author:* Tel.: +31 20 512 2792; fax: +31 20 512 2799.
E-mail address: o.v.tellingen@nki.nl (O. van Tellingen).
0959-8049/$ - see front matter
doi:10.1016/j.ejca.2006.07.013

1. Introduction

The brain is effectively protected against harmful substances by the blood–brain barrier (BBB). This barrier is considered the major reason for the limited success of systemic chemotherapy in the treatment of patients with primary brain tumours. A hallmark of primary brain tumours is their ability to infiltrate into the surrounding normal brain tissue. Although the BBB is usually leaky in the central part of the tumour, the peripheral parts and cells that infiltrate into the surrounding tissue are protected by the normal BBB and are, therefore, poorly accessible for chemotherapy. Strategies to improve the access and efficacy of chemotherapy include bypassing or disruption of the BBB[1,2] or use of agents that more easily penetrate the BBB.[3,4] A rational step prior to clinical testing of these strategies and agents is to establish their efficacy against intracranial tumour models in laboratory animals.

Traditionally, mouse models for brain cancer are established by intracranial injection of tumour cells.[5] Intracranial tumour injection can be done successfully in mice although, because of their size, rats are also extensively used for this type of experiments. Typically, tumour cells originally derived from patients suffering from malignant glioma, for example the U87MG cell-line, are being used. Although these tumour models are generally considered orthotopic models of brain cancer, the histology of the tumours that emerge from these human xenografts is usually very distinct from that of patient tumours. In particular, many of these tumours grow in uniform massive 'ball-like' structures, without infiltration of surrounding tissue. Moreover, because the BBB is more or less uniformly disrupted throughout these lesions, testing of chemotherapeutic agents likely results in an over-estimation of their efficacies. In order to include the issue of limited drug delivery in experimental chemotherapy efficacy studies against intracranial tumours, the use of tumour models that grow behind an intact BBB is pivotal. This paper describes the development of a panel of intracranially growing tumour models that, despite the fact that not all cell lines were derived of primary brain tumours, mimic the variations in growth characteristics of brain tumours in patients more closely. To establish the BBB properties of the different models, we used immunohistochemistry and contrast enhanced magnetic resonance imaging (CE-MRI). All the cell lines highly express the firefly protein luciferase to allow convenient non-invasive *in vivo* follow up of the tumour growth during chemotherapy efficacy studies.

2. Methods

2.1. Animals

Experiments were carried out in athymic male and female FVB mice between 8 and 12 weeks of age. The mice were bred in our institute and maintained in filtertop cages with free access to food and water and they were handled in laminar airflow. The animal experiment committee approved these experiments.

2.2. Tumour cell lines and transfections

Cell lines were cultured in MEM (Life Technologies Inc., Breda, The Netherlands) supplemented with 10% foetal calf serum, non-essential amino acids, streptomycin, penicillin and sodium pyruvate (all Life Technologies), and incubated at 37 °C and 5% CO_2 in humidified air. The human U87MG and the rat RG-2 glioblastoma cell lines were obtained from the American Type Culture Collection (ATCC, Rockville, USA). The human breast cancer cell line MDAMB 435 and the murine melanoma cell line K1735SW1 were kindly provided by Dr. I.J. Fidler (MD Anderson Cancer Center, Houston, USA). The K1735Br2 cell line was obtained after two successive *in vivo* passages in FVB/nude mice after intracarotid injection of 1×10^5 K1735SW1 tumour cells.[6] The Mel57 (University Medical Centre, Nijmegen, The Netherlands) is a human melanoma cell line and the Mel57VEGF subline was obtained by transfection of the Mel57 cell line with $VEGF_{165}$.[7]

All cell lines were further transfected by standard protocols with lipofectamine using a pBS vector containing an β-actin driven luciferase gene coupled *via* an internal ribosome expression site to GFP. After expansion, GFP bright cells were sorted to single cells by FACS, expanded and sublines tested for luciferase expression by an *in vitro* bioluminescence assay (Promega, Benelux BV, Leiden, The Netherlands). Three to five sublines of each cell line showing the highest luminescence activity were tested *in vivo* for tumour take and intracranial growth behaviour.

To retrieve tumour cells for injection, cell cultures were trypsinised (trypsin 0.05%; EDTA 0.02%, Life Technologies), washed two times with Hanks Balanced Saline Solution (HBSS, Life Technologies Inc.), counted and resuspended in an appropriate volume of HBSS. The single cell suspensions were kept on ice until injection.

2.3. Cerebral injection procedure

Mice were anaesthetised by intraperitoneal injection of 6 ml/kg of a 1:1:2 (v/v/v) mixture of Hypnorm (fentanyl 0.2 mg/ml and fluanisone 10 mg/ml; Jansen Cilag, Tilburg, The Netherlands), Dormicum (midazolam 5 mg/ml; Rôche Nederland, Mijdrecht, The Netherlands) and water for injection (Braun, Emmer-Compascuum, The Netherlands). Mice were placed in a stereotact (ASI instruments, Warren, MI, US). After preparation of the skull a small hole of 1 mm in diameter was drilled at 2 mm lateral and 1 mm anterior to the bregma, because this was shown a reliable place for tumour engraftment.[8] The 30-gauge needle was attached to a 50 μl syringe (Hamilton Bonaduz AG, Bonaduz, Switzerland) and fitted in an infusion pump (Baby Bee Syringe Drive (BAS Instruments Ltd. Warwickshire, UK)). The needle was inserted 3 mm below the skull surface and we injected 2 μl of a cell suspension containing 5×10^3–1×10^5 cells, depending on the cell line, at a rate of 0.4 μl/min.

2.4. Bioluminescence imaging

Tumour bearing animals were injected i.p. with 150 mg/kg luciferin (Xenogen Corp., Alameda, CA, USA) in PBS. After

10 min the mice were anaesthetised with 2% isofluorane (Forene®, Abbott Laboratories Ltd., Queenborough, United Kingdom)/air mixture and placed in a dark box under the cryogenically cooled IVIS camera (Xenogen Corp.). During image recording, mice inhaled isofluorane delivered *via* a nose cone and their body temperature was maintained at 37 °C in the dark box of the camera system. Bioluminescence images were recorded between 10 and 20 min post luciferin administration.[9] Mice recovered from anaesthesia within 2 min after imaging. The bioluminescence intensity was quantified with the LivingImage software (Xenogen Corp.) as an overlay on IGOR (Wavemetrics, Seattle, WA, USA). Signal intensity was quantified as the sum of detected photons per second within the region of interest using the LivingImage software package.

By using the *in vitro* Promega bioluminescence assay, the *ex vivo* bioluminescence was measured in U87MG tumours isolated from the brain that were lysed/homogenised in the cell lysis buffer provided in the Promega kit and the *ex vivo* intensity was compared with the *in vivo* signal at the day of sacrifice.

2.5. CE-MRI imaging

Contrast enhanced magnetic resonance imaging (CE-MRI) was performed at 2–4 weeks after tumour cell implantation using gadolinium diethyl-enetriaminepenta-acetic acid (Gd-DTPA) to detect vascular leakage, i.e. BBB disruption. Images were acquired before, directly post and 2 and 10 min post-injection of i.v. 0.2 mmol/kg Gd-DTPA (Magnevist®, Schering, Germany) with a T_1-weighed multisence gradient-echo sequence (T_r = 40 ms, T_e = 7 ms) (for details see Ref. [10]). At least two mice per model were used.

2.6. Histological and immunohistochemical analysis

Mice were sacrificed about 2–4 weeks after tumour cell injection. Brain tissue was fixed in formalin, embedded in paraffin and cut in coronal slices of 4 μm. The sections were H&E stained. For immunohistochemistry, the slices were processed as described previously.[7] The primary antibodies used were rabbit anti-mouse Ki-67 (Dianova, Hamburg, Germany) and anti-Glut-1 (Dako, Glostrup, Denmark). Integrity of the BBB was also investigated by staining for extravasated mouse immunoglobulins.[11]

2.7. Applicability for drug screening

Three cohorts of mice each were intracranially injected with luciferase-labelled U87MG (n = 20), Mel57 (n = 17) or RG-2 (n = 18) tumour cells. Seven days later, bioluminescence images were taken and animals were stratified into the treatment group or the control group. Animals that have a bioluminescence reading, which is very different from the group mean, can be eliminated from the study at this point. Therapy was started and consisted of oral temozolomide given at a dose of 100 mg/kg/day for five subsequent days. For this purpose, the contents of a 20 mg capsule were dissolved in 4 ml of 5% Ethanol in saline by sonication for 5 min. Next, following centrifugation the supernatant was filtered through a 0.2 μm filter (Millipore, Bedford, MA, USA). The final concentration was 5 mg/ml and was administered at 20 μl per gram body weight. The contents of one capsule suffice for the treatment of about eight animals. Bioluminescence images were taken at least every week for follow up of tumour growth. The experiments were terminated before or as soon as the first animals in a group developed disease-related symptoms.

3. Results

3.1. Growth characterisation of cell lines in vivo

Intracranial tumours were generated by stereotactic injection of the different cell lines into the caudate putamen (striatum) of the brain. In order to minimise local effects (stress/damage) on the normal brain tissue surrounding the injection site we have minimised the injection volume as much as practically feasible. Moreover, we implemented the use of an infusion pump driven syringe allowing injection at a very low flow rate of 0.4 μl/min, thus leaving more time for the injected fluid to diffuse away into the extracellular space. Our experience using this setup with any of these tumour cell lines ranges from at least 50 to several hundred injections. Tumour take in the brain usually occurs in more than 95% of the animals, indicating that the brain is a fertile soil for these tumours cells. In general, disease related symptoms developed in about 4 weeks after injection of the cells and large tumour lesions were found at the site of injection. Injection of 1×10^5 cells resulted in reproducible tumour growth with all of the cell lines. However, injection of 1×10^5 Mel57VEGF cells resulted in death of all the injected mice within five days. Morphological examination showed extensive brain oedema, which was probably the main cause of death. Reducing the number of injected cells to 5×10^3 of Mel57VEGF cells gave reproducible growth and tumours that were lethal after about 4 weeks. Similarly, we reduced the number of RG-2 cells to 5×10^3 per injection. This window of 4 weeks is convenient for most chemotherapy efficacy studies.

The K1735Br2 cell line shows a very profound infiltration of the surrounding brain tissue, similar to the growth pattern observed after intracarotid arterial injection of the K1735SW1 parental cell line[6] (Fig. 1). Numerous cords of tumour cells that cluster along the existing blood vessels at far distances from the centre of the tumour are present. The blood vessels appear to be similar as in the normal brain parenchyma; however, in some parts of the tumour some dilatation of vessels was observed. The K1735Br2 lesions grew throughout the parenchyma of the affected hemisphere, but occasionally also along the needle track into the meninges. The Mel57 parental tumour shows some invasion of cells into the surrounding parenchyma, although to a much lesser magnitude than that observed with K1735Br2. Moreover, this infiltration becomes even less visible when more bulky lesion had formed. The vessel density in the Mel57 tumours is relatively low and especially in larger, more advanced tumours rather extensive necrosis at the more central parts can be observed. Necrosis is also found in advanced MDAMB435 brain tumours, whereas Mel57VEGF and U87MG are well vascularised growing expansively to large lesions without necrosis. The rat glioma cell line RG-2 grows rather infiltrative / invasive in the brain of mice thus maintaining the reported growth behaviour when stereotactically injected into the brain of syngeneic rats.[12]

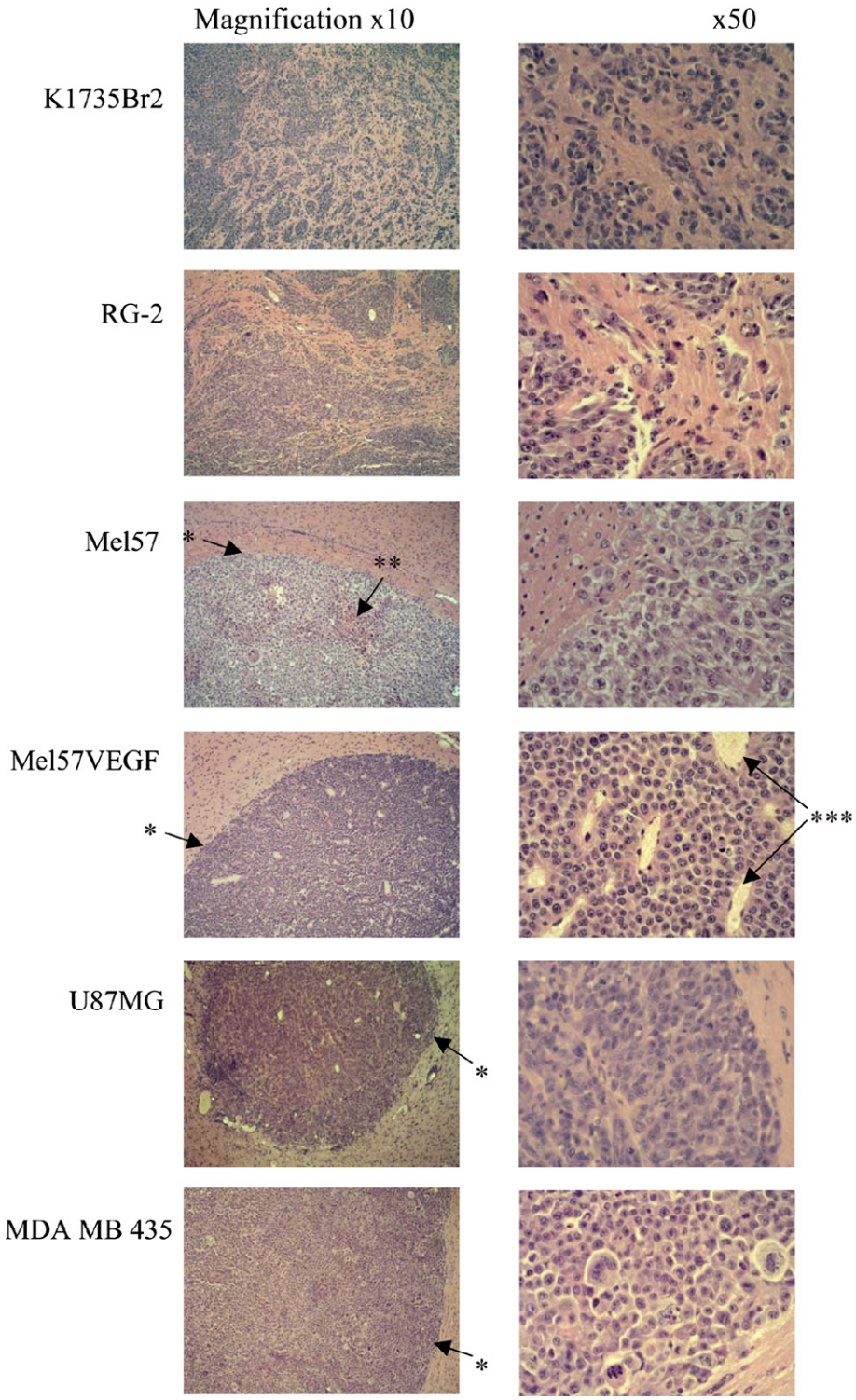

Fig. 1 – Histological properties of intracranial tumours growing after stereotactic implantation. Whereas K1735Br2 and, to a lesser extend RG-2 tumour cells invade into the parenchyma, other tumours develop into more compact lesions with clear margins (*). Necrosis was generally observed in late stage lesions of Mel57 (**) and MDA MB435 but never in U87MG and Mel57VEGF. Especially the latter tumour contained many large blood vessels (***). (Hematoxylin and eosin stained sections).

3.2. *CE-MRI imaging of intracranial tumours*

We have used CE-MRI using Gd-DTPA to establish the vascular leakage in tumours in the brain. The images were taken pre- and post-administration of Gd-DTPA and were obtained two to four weeks after injection of the tumour cells (Fig. 2). In the coronal images the tumours are present in the right hemisphere and are slightly visible before administration of the

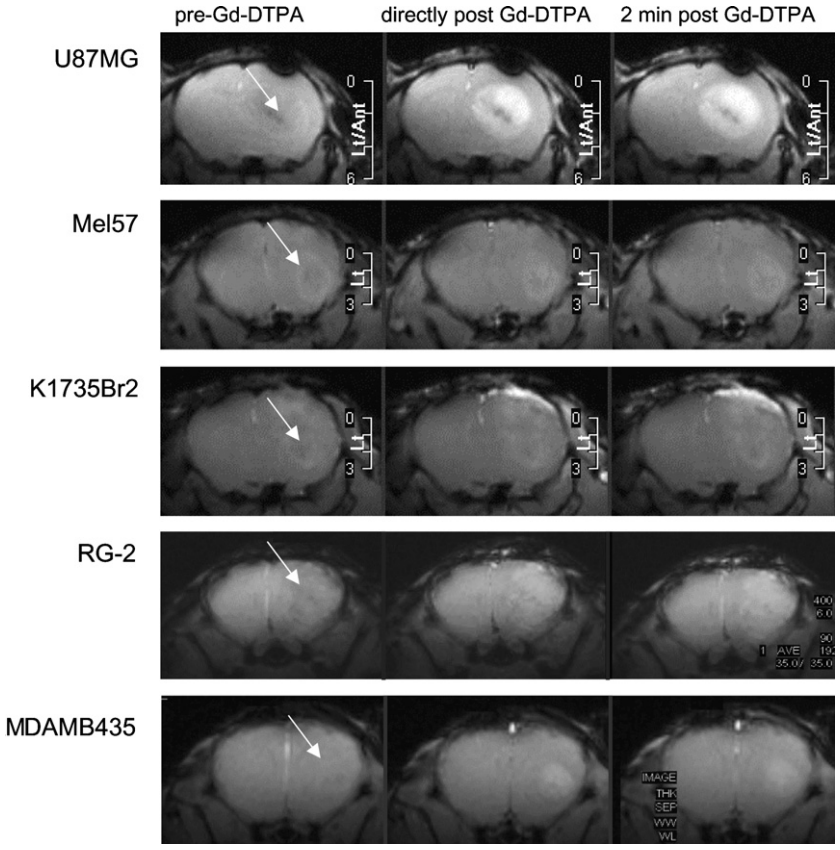

Fig. 2 – Contrast enhanced-MRI of mouse brains with tumours of K1735Br2, Mel57, U87MG, RG-2 and MDA MB435. The images were taken before and directly and 2 min post-injection of the contrast agent Gd-DTPA. The arrows indicate the locations of the lesions. The strong enhancement after injection of the contrasting agent in case of U87MG tumours visualises the profound leakiness of the vasculature. The enhancement in the other tumours was much less. Some enhancement was observed in MDA MB 435 tumours although this image was already taken 14 days after tumour cell injection when the lesion was still fairly small. All other tumours in this figure were more advanced as cells had been injected 3–4 weeks before MR-imaging.

contrast fluid. In the pre-contrast image of the U87MG tumour, a hypointense area was seen, possibly due to some oedema. Administration of Gd-DTPA resulted in a clear enhancement of the contrast within the U87MG tumour followed by rapid washout at 10 min post Gd-DTPA (not shown), which is typical for vascular leakage of Gd-DTPA into the tumour. In case of Mel57, only very small differences were seen between the pre- and post-contrast images even in this bulky lesion. This is similar as in a previous report when cells grew after injection into the carotid artery.[10] Only a very minor enhancement of contrast was observed in the centre of the tumour, which had disappeared at 10 min post-contrast (not shown). Similarly, bulky lesions of RG-2 tumours were non-leaky to the contrasting agent. In case of K1735Br2, there is an asymmetry between the left and right hemisphere and it is obvious that there is a clear mass effect of the tumour in the right hemisphere. No enhancement was observed in the centre of the tumour that grows within the brain parenchyma, when comparing the pre- and post-contrast images. However, in this animal suffering from late-stage disease, leakage of Gd-GTPA occurred near the meninges of the involved hemisphere. This may be due to a reactive or angiogenic response as a consequence of serious local tumour growth in the meninges. MDA MB 435 tumours were invisible on MRI when they were small in size. However, by day 14 after injection we observed leakiness of the vasculature.

3.3. *Immunohistochemistry*

The cell lines U87MG, Mel57 and K1735Br2 were examined by immunohistochemical analyses (Fig. 3). Staining for mouse immunoglobulins showed substantial diffusion of IgG surrounding the U87MG lesions, indicative of a permeable vasculature. Much less extravasation of IgG was detected in the Mel57 and K1735Br2 lesions. The staining for Glut-1, a marker of the BBB, was found in the endothelial cells in all tumours, but the staining appears less intense in slides of Mel57 tumours because of the lower vessel density (Fig. 3). Somewhat surprisingly, a substantial expression of Glut-1 was also detected in the leaky vessels of U87MG tumours that are most likely not of pre-existing nature. As Glut-1 is considered a marker for the BBB, it may be that astrocyte-endothelial interactions have induced the expression of brain endothelial differentiation markers such as Glut-1 in these newly formed endothelial cells.[13] The astrocytic characteristics of the

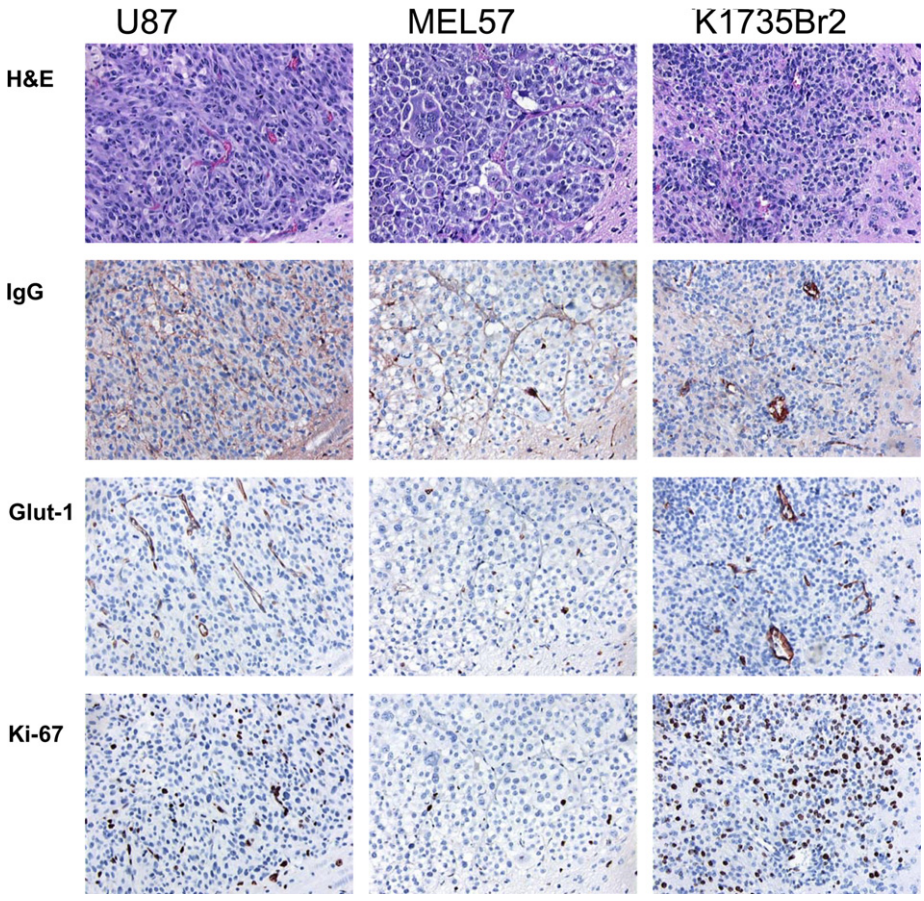

Fig. 3 – Immunohistochemical growth patterns of U87MG, Mel57 and K1735Br2 lesions in the brain. The substantial IgG staining in and around U87MG lesions correlates with the leakiness of the blood vessels. The vessel density in U87 was relatively high and vessels stained positive for the BBB marker Glut-1. Vessel density was lower in Mel57 and K1735Br2. Typically, cords of K1735Br2 tumour cells proliferated around the blood vessels. The staining for Ki67 showed numerous proliferating endothelial cells in U87MG but only very few in Mel57. In case of the murine K1735Br2 tumour cells also stained positive for Ki67.

U87MG cell line may therefore be an explanation for the Glut-1 staining in these lesions.

Staining for the murine nuclear antigen Ki-67 (Fig. 3) showed proliferation of endothelial cells and pericytes in the U87MG lesion. In contrast, staining with Ki-67 in Mel57 tumours was much less. In case of K1735Br2, which is a tumour cell line of murine origin, the proliferating tumour cells were also stained.

3.4. *In vivo imaging of intracranial tumours with luciferase*

To allow non-invasive monitoring of intracranial tumours, we have created sublines that strongly express the firefly protein luciferase under the actin promoter. At least three transfected sublines of each cell line were selected based on their *in vitro* growth characteristics and *in vitro* bioluminescence activity and used for *in vivo* testing. Most of these sublines mimicked the *in vivo* growth characteristics of the orginal cell line. From these, one subline of each cell line was selected for further efficacy studies.

We determined the optimum lag-time between the injection of luciferin and acquisition of the bioluminescence signal (Fig. 4C). After an initial increase of the signal a plateau was reached within 10–15 min after i.p. injection of luciferin, which remained constant for more than 15 min allowing a convenient window for acquiring bioluminescence images. In a separate work that we performed using the K1735Br2 tumour cell line in a lung metastasis model, we have observed similar time–response curves (see example in Fig 4C), suggesting that the intensity of the bioluminescence signal is determined by the rate at which luciferin reaches the systemic circulation from the peritoneal cavity and that the BBB does not further delay the response of the signal.

Fig. 4A depicts the time course of bioluminescence intensities after stereotactic injection of 1×10^5 U87MG tumour cells into the brain. Already 4 days after tumour cell injection a clear signal was detected, and following an initial lag time of about 1 week the signal increased by more than 60-fold at day 25. In the case of Mel57VEGF tumour cells, the signal increased immediately from day 4 onwards (Fig. 4B). Overall the variation in tumour growth between the animals in these

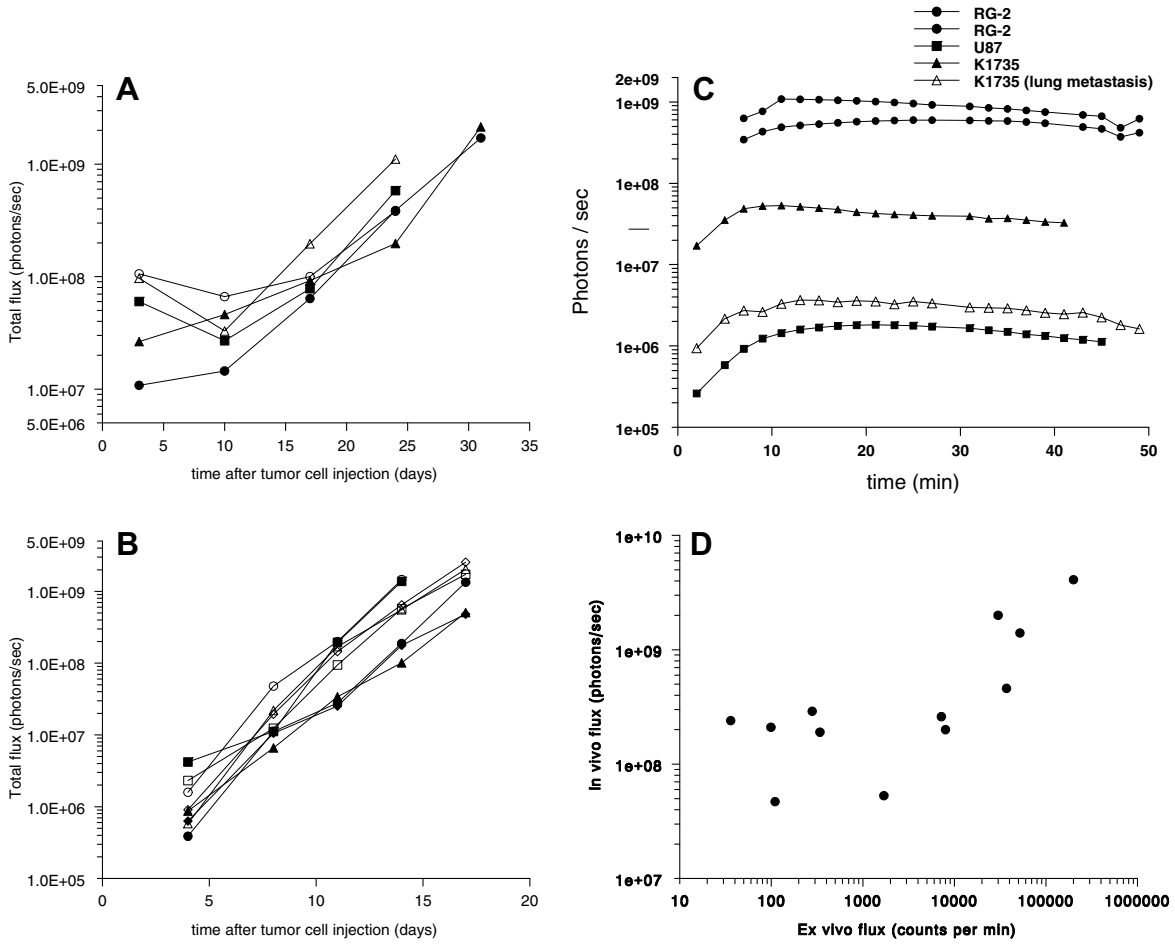

Fig. 4 – Measurement of bioluminescence of brain tumours. Patterns of the bioluminescence are shown after stereotactic injection of 1×10^5 U87MG (A, $n = 5$ mice) and 5×10^3 Mel57VEGF (B, $n = 8$ mice) tumour cells into the brain. Each curve represents the course of the bioluminescence intensity observed per animal. The curves show that Mel57VEGF tumours proliferate from early on, whereas there is a lag time in case of U87MG cells. The photon flux of intracranial tumours following the i.p. injection of luciferin increases during the first 15 min and then remains relatively stable for another 15–20 min leaving a convenient window for imaging (C). This same pattern was observed with extracranial tumours (lung metastasis model), suggesting that the bioluminescence signal is determined by the release of luciferin from the peritoneal cavity into the systemic circulation rather than by BBB passage. There was a significant correlation ($r = 0.73$, $p < 0.05$) between *in vivo* bioluminescence imaging and *ex vivo* bioluminescence determinations (D).

intracranial models is very similar to what might be expected after subcutaneous xenografts. The increase in bioluminescence intensity was accompanied with an increase in tumour mass, as confirmed by histology as well as by the *ex vivo* bioluminescence in lysates of isolated tumours measured using the *in vitro* Promega assay kit ($r = 0.73$). More important than this correlation, however, is the fact that a very reasonable number of animals (typically 8–9 mice per cohort; test group *versus* control group) will be sufficient to record a meaningful response before animals will experience disease-related discomfort.

3.5. *Applicability for chemotherapy efficacy studies*

In order to demonstrate the applicability of our models for *in vivo* drug screening, we performed a series of experiments in U87MG, Mel57, RG-2 and K735Br2 using the anti-cancer agent temozolomide (TMZ). TMZ drug is approved for the treatment of (recurrent) anaplastic astrocytomas and glioblastoma multiforme, as single agent or in combination with radiotherapy and has modest activity prolonging the life of patients suffering from this devastating disease with very dismal prognosis by several months.[14,15] We have tested TMZ given as daily oral doses of 100 mg/kg for five subsequent days. The responses that we observed differed substantially between the tumour models. On the one hand, the response in U87MG is dramatic, even resulting in cures in some animals, whereas on the other hand, the RG-2 tumour did not demonstrate a significant response (Fig. 5). Although the relative sensitivities of the tumour cell lines towards TMZ will also determine the success of TMZ chemotherapy, the much more profound leakiness of the blood vessels in intracranial U87MG tumours *versus* the other tumour models used in this experiment is most likely an important factor.

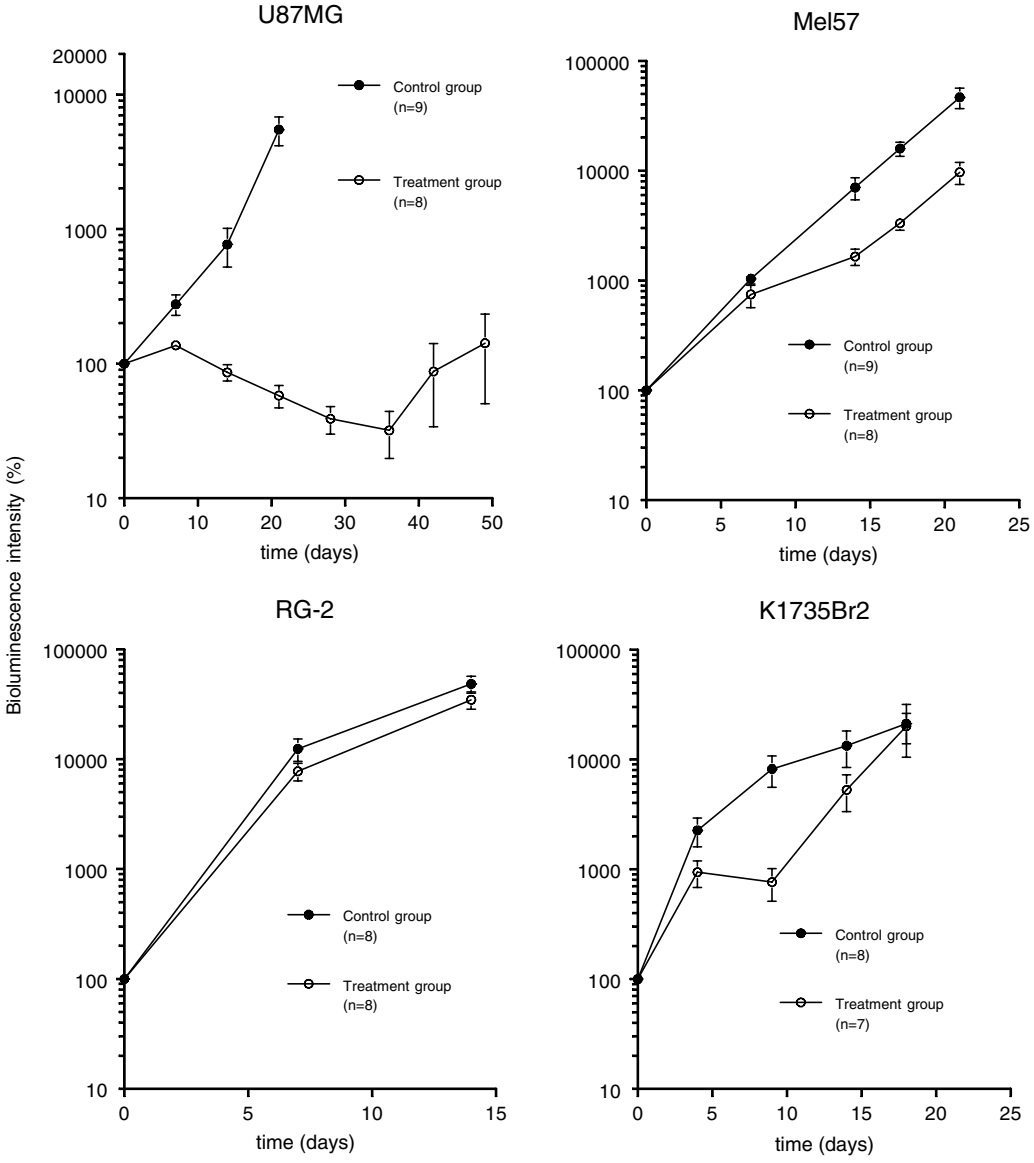

Fig. 5 – Antitumour efficacy of temozolomide. Animals bearing U87MG, Mel57, RG-2 or K1735Br2 tumours received temozolomide 100 mg/kg/day × 5 (treatment groups) or no treatment (control groups) starting from day 7 after tumour cell injection. Bioluminescence imaging was performed at the start of treatment (day 0) and at least every week thereafter. Values were plotted relative to the image taken at day 0, which was arbitrarily set at 100%.

4. Discussion

We have developed a range of intracranial tumour models, which display the typical infiltrative, invasive and expansive growth patterns as seen in patients suffering from brain cancer. Importantly, these growth characteristics were accompanied by differences in the permeability of the BBB in those tumours. Furthermore, we have successfully implemented the use of non-invasive monitoring of the tumour growth by using luciferase transfected cell lines, making these models particularly useful for chemotherapy intervention studies.

Tumour progression in the brain may induce angiogenesis to meet the demands for nutrition and oxygenation and the newly formed vessels generally do not display the BBB properties that are characteristic for normal brain vasculature.[16] However, brain tumours may also expand through co-option of the existing blood vessels and by invasion of brain parenchyma, and in these situations the BBB properties may be much better maintained.[17] Similarly, many extracranial tumours metastasise to the brain at high frequency and as long as they have not yet reached a size that mandates the formation of new blood vessels, they will essentially grow behind an intact BBB.[18] It is likely due to the presence of a relatively intact BBB that systemic chemotherapy is barely effective against brain tumours, except for the treatment of the larger metastatic lesions.[19]

The majority of preclinical efficacy studies performed to date have utilised glioma derived cell lines, such as the

U87MG.[20] However, most of these tumours usually grow expansively as uniform 'ball-like' structures in the brain. As shown by using CE-MRI, the vessels in U87MG tumours are very leaky and, consequently, all parts of the tumour are readily accessible to systemic drug treatment. This lack of a barrier causes that such models will over-predict the efficacy of an agent and may thus explain why agents that were active in preclinical studies have failed to work in patients. This was clearly illustrated by our results with TMZ chemotherapy. Although TMZ has activity against brain cancer, cures are unfortunately not achieved in patients when using this drug. The response of TMZ against intracranial lesions that do possess a more intact barrier is much less pronounced. Although differences in the relative sensitivities towards TMZ between the different cell lines may also be a factor underlying the observed differences in response, this could not be verified by simple *in vitro* cytotoxicity testing. In spite of the apparent potency of TMZ *in vivo*, this drug is not very active in vitro. In line with others[21,22], we had to use concentrations far above 100 μM in order to observe notable cell kill of U87MG by TMZ (results not shown). The reason for this discrepancy between *in vitro* and *in vivo* potency is not clear, but might be related to the fact that TMZ is a prodrug that requires a conversion into 3-methyl-(triazen-1-yl)imidazole-4-carboximide,[14] which might occur less efficiently *in vitro* than *in vivo*. Clearly, the relevance of *in vitro* cytotoxicity testing using concentrations far above those that can be achieved *in vivo* is obscure.

Brain metastases that respond to chemotherapy[19] most likely have a leaky vasculature and may be well mimicked by the preclinical models such as MDA MB 435 and Mel57-VEGF. In all other cases, expansively growing tumours with leaky vessels are not the appropriate models to be used in chemotherapy intervention studies, as an intact BBB structure is an essential feature of those tumours. The K1735Br2, Mel57 and RG-2 lesions appear to fulfill these demands, as there was no leakage of Gd-DTPA. Histological analysis demonstrated that the K1735Br2 cell line grows mainly through co-optation of the existing brain capillaries, and based on MRI and IgG staining the BBB in these tumours is virtually intact. The Mel57 also grow into invasively although to a much lesser extent as K1735Br2. Moreover, necrosis was evident in some areas of the tumour when the Mel57 tumours grows to larger lesions, which is usually not seen in Mel57 brain metastases growing after injection of the cells into the carotid artery.[7,10] Most likely, this difference is due to the fact that multiple smaller lesions originating from single cells occur after intra-carotid arterial injection, whereas tumours develop from a deposit of tumour cells in our stereotactic model. Nevertheless, even when developed into large lesions the blood vessels in Mel57 tumours maintain non-leaky BBB characteristics. Thus, although the K1735Br2 and Mel57 cell lines do not originate from a primary brain tumour, they may be more appropriate for pharmacological studies testing drug penetration and efficacy in brain tumours than some of the more generally used human glioblastoma-derived cell lines. The RG-2, however, appears to be a good primary brain tumour model with respect to permeability of the BBB, albeit that this is a rat and not a human derived cell line.

Thus far, therapeutic intervention studies with preclinical brain tumour model have been performed using survival time supplemented by histological confirmation as read-out for efficacy. The statistical power of such methods is rather poor, because the tumour take and size of the tumour are unknown at the time of therapeutic intervention. Consequently, large numbers of animals are required which will also be exposed to considerable discomfort, because symptoms of illness and survival time are used as read-out. Recent studies have already shown the benefits of bioluminescence imaging of xenografts comprising stably transfected cell lines expressing the firefly luciferase as a convenient and sensitive non-invasive technique to determine tumour burden in deeply situated tissues.[23] In the present study, we have implemented this technique for our brain tumour models. Injection of the luciferase tagged sublines resulted in reproducible tumour models, while maintaining the salient morphological characteristics of the parental line. A major advantage is that the imaging procedure by itself causes only very moderate discomfort to the animal and can be repeated several times, which allows follow up of the tumour burden during and after the treatment.

Obviously, mouse models that may recapitulate the infiltrative and other typical characteristics of human glioma even better might be obtained by using conditional transgenic and/or knockout mice for relevant tumour promoter and suppressor genes or by somatic cell gene transfer using retroviral vectors to the neonatal mouse brain.[24,25] Such models have already made a considerable contribution to the understanding of the biology and development of brain tumours. Furthermore, they are promising with respect to the development of more clinically relevant experimental tumour models for therapeutic studies. Thus far, however, the implementation of these models for this purpose is not yet practical due to the lack of models that are sufficiently reproducible in tumour onset and growth rate.

In conclusion, the use of luciferase tagged tumour cells in intracranial xenografts provides a convenient and powerful tool for non-invasive *in vivo* monitoring of intracranial tumours. Their implementation in (chemo)therapy-efficacy studies will reduce the number of animals and the degree of discomfort. Moreover, we expect that our brain tumour models with an intact BBB structure will be a valuable improvement compared to the existing models that are currently used to test the efficacy of anticancer agents against brain tumours.

Conflict of interest statement

None declared.

Acknowledgement

This work was supported by Grants NKI99-2033 and KUN00-2302 from the Dutch Cancer Society, ZonMw Grant 3170.0056 and NWO Grant 920-03-149.

REFERENCES

1. Kemper EM, Boogerd W, Thuis I, Beijnen JH, van Tellingen O. Modulation of the blood–brain barrier in oncology:

therapeutic opportunities for the treatment of brain tumours? *Cancer Treat Rev* 2004;**30**:415–23.
2. Bart J, Groen HJ, Hendrikse NH, van der Graaf WT, Vaalburg W, de Vries EG. The blood–brain barrier and oncology: new insights into function and modulation. *Cancer Treat Rev* 2000;**26**:449–62.
3. Levin VA, Prados MD. Treatment of recurrent gliomas and metastatic brain tumours with a polydrug protocol designed to combat nitrosourea resistance. *J Clin Oncol* 1992;**10**:766–71.
4. Yung WK, Albright RE, Olson J, et al. A phase II study of temozolomide *vs*. procarbazine in patients with glioblastoma multiforme at first relapse. *Br J Cancer* 2000;**83**:588–93.
5. Peterson DL, Sheridan PJ, Brown Jr WE. Animal models for brain tumours historical perspectives and future directions. *J Neurosurg* 1994;**80**:865–76.
6. Schackert G, Fidler IJ. Development of *in vivo* models for studies of brain metastasis. *Int J Cancer* 1988;**41**:589–94.
7. Kusters B, de Waal RM, Wesseling P, et al. Differential effects of vascular endothelial growth factor a isoforms in a mouse brain metastasis model of human melanoma. *Cancer Res* 2003;**63**:5408–13.
8. Lal S, Lacroix M, Tofilon P, Fuller GN, Sawaya R, Lang FF. An implantable guide-screw system for brain tumour studies in small animals. *J Neurosurg* 2000;**92**:326–33.
9. Contag CH, Spilman SD, Contag PR, et al. Visualizing gene expression in living mammals using a bioluminescent reporter. *Photochem Photobiol* 1997;**66**:523–31.
10. Leenders W, Kusters B, Pikkemaat J, et al. Vascular endothelial growth factor-A determines detectability of experimental melanoma brain metastasis in GD-DTPA-enhanced MRI. *Int J Cancer* 2003;**105**:437–43.
11. Proescholdt MA, Heiss JD, Walbridge S, et al. Vascular endothelial growth factor (VEGF) modulates vascular permeability and inflammation in rat brain. *J Neuropathol Exp Neurol* 1999;**58**:613–27.
12. Barth RF. Rat brain tumour models in experimental neuro-oncology: the 9L, C6, T9, F98, RG2 (D74), RT-2 and CNS-1 gliomas. *J Neurooncol* 1998;**36**:91–102.
13. Regina A, Morchoisne S, Borson ND, McCall AL, Drewes LR, Roux F. Factor(s) released by glucose-deprived astrocytes enhance glucose transporter expression and activity in rat brain endothelial cells. *Biochim Biophys Acta* 2001;**1540**:233–42.
14. Yung WK. Temozolomide in malignant gliomas. *Semin Oncol* 2000;**27**:27–34.
15. Stupp R, Mason WP, van den Bent MJ, et al. Radiotherapy plus concomitant and adjuvant temozolomide for glioblastoma. *N Engl J Med* 2005;**352**:987–96.
16. Plate KH, Risau W. Angiogenesis in malignant gliomas. *Glia* 1995;**15**:339–47.
17. Leenders WP, Kusters B, de Waal RM. Vessel co-option: how tumours obtain blood supply in the absence of sprouting angiogenesis. *Endothelium* 2002;**9**:83–7.
18. Fidler IJ, Yano S, Zhang RD, Fujimaki T, Bucana CD. The seed and soil hypothesis: vascularisation and brain metastases. *Lancet Oncol* 2002;**3**:53–7.
19. van den Bent MJ. The role of chemotherapy in brain metastases. *Eur J Cancer* 2003;**39**:2114–20.
20. Abernathey CD, Kooistra KL, Wilcox GL, Laws Jr ER. New xenograft model for assessing experimental therapy of central nervous system tumours: human glioblastoma in the intrathecal compartment of the nude mouse. *Neurosurgery* 1988;**22**:877–81.
21. Sankar A, Thomas DG, Darling JL. Sensitivity of short-term cultures derived from human malignant glioma to the anti-cancer drug temozolomide. *Anticancer Drugs* 1999;**10**:179–85.
22. Eyupoglu IY, Hahnen E, Trankle C, et al. Experimental therapy of malignant gliomas using the inhibitor of histone deacetylase MS-275. *Mol Cancer Ther* 2006;**5**:1248–55.
23. Edinger M, Cao YA, Hornig YS, et al. Advancing animal models of neoplasia through *in vivo* bioluminescence imaging. *Eur J Cancer* 2002;**38**:2128–36.
24. Holland EC, Hively WP, DePinho RA, Varmus HE. A constitutively active epidermal growth factor receptor cooperates with disruption of G1 cell-cycle arrest pathways to induce glioma-like lesions in mice. *Genes Dev* 1998;**12**:3675–85.
25. Uhrbom L, Hesselager G, Nister M, Westermark B. Induction of brain tumours in mice using a recombinant platelet-derived growth factor B-chain retrovirus. *Cancer Res* 1998;**58**:5275–9.